Clays and Clay Minerals, Vol. 42, No. 4, 369–381, 1994.

THE DIAGENETIC TO LOW-GRADE METAMORPHIC EVOLUTION OF MATRIX WHITE MICAS IN THE SYSTEM MUSCOVITE-PARAGONITE IN A MUDROCK FROM CENTRAL WALES, UNITED KINGDOM*

GEJING LI,[1] DONALD R. PEACOR,[1] R. J. MERRIMAN,[2] AND B. ROBERTS[3]

[1] Department of Geological Sciences, University of Michigan
Ann Arbor, Michigan 48109-1063

[2] British Geological Survey, Keyworth, Nottingham NG12 5GG, United Kingdom

[3] Geology Department, Birkbeck College, Malet Street, London WC1E 7HX, United Kingdom

Abstract—Two orientations of white micas with subordinate chlorite have been observed in a fine-grained (50 Å to 2 μm) matrix of a Silurian lower anchizonal mudrock from central Wales: one parallel to bedding and one parallel to cleavage that is approximately 30°–50° to bedding. Bedding-parallel micas consist of small (50–200 Å thick) deformed packets ($1M_d$ polytype) and larger (100 Å–2 μm) strain-free grains ($2M_1$ polytype). All strained micas and some strain-free grains have compositions varying from $Mu_{86}Pg_{14}$ to $Mu_{58}Pg_{42}$, intermediate to muscovite and paragonite, and falling within the Mu-Pg solvus. Individual packets of layers are chemically homogeneous and some of them give only one set of 00*l* reflections (d ≈ 19.6 Å). Micas with such intermediate compositions are metastable. Some packets of coarse, strain-free micas have compositions of approximately $Mu_{93}Pg_7$ or $Mu_{11}Pg_{89}$. Split pairs of 00*l* reflections with d-values of 20 Å and 19.6 Å, and 20 Å and 19.2 Å, respectively, were observed in some SAED patterns, suggesting coexistence of muscovite and intermediate Na/K mica (~$Mu_{60}Pg_{40}$), and of discrete muscovite and paragonite, consistent with the splitting of the basal reflections of micas as observed in bulk-rock XRD patterns. Cleavage-parallel micas ($2M_1$ and 3T polytypes) occur as strain-free large grains (200 Å to 2 μm) of discrete muscovite ($Mu_{100}Pg_0$) and paragonite (Mu_6Pg_{94}), often with subhedral to euhedral cross-sections.

The data suggest that bedding-parallel metastable micas with disordered interlayer K and Na were initially derived from alteration of smectite during burial diagenesis. They subsequently underwent dissolution, with crystallization of more evolved bedding-parallel micas during deep burial. Discrete grains of stable muscovite and paragonite then crystallized in the cleavage orientation through tectonic stress-induced dissolution of bedding-parallel matrix micas. Combined XRD and TEM/AEM data further show that the so-called 6:4 ordered mixed-layer paragonite/muscovite actually corresponds to cation-disordered, homogeneous mica of intermediate composition.

Key Words—Central Welsh basin, Diagenesis, Intermediate Na/K mica, Low-grade metamorphism, Modulated structure, Muscovite, Paragonite, Solvus.

INTRODUCTION

Micas having compositions within the solid solution series muscovite [$KAl_2Si_3AlO_{10}(OH)_2$]-paragonite [$NaAl_2Si_3AlO_{10}(OH)_2$] occur in prograde metamorphic rocks that range in grade from late diagenesis through the anchizone to the epizone (Frey, 1969, 1970, 1978, 1987; Livi *et al.*, 1988, 1990), including the prehnite-pumpellyite and pumpellyite-actinolite facies (Merriman and Roberts, 1985; Pe-Piper, 1985), and to middle grade metamorphic rocks (Guidotti, 1984; Essene, 1989; Shau *et al.*, 1991, and references therein). The degree of solid solution in coexisting muscovite (Mu) and paragonite (Pg) has been shown to increase with increasing grade and, therefore, with temperature in natural rock systems (Rosenfeld *et al.*, 1958; Zen and Albee, 1964) and in syntheses (e.g., Fujii, 1966; Popov, 1968; Blencoe and Luth, 1973; Blencoe, 1974; Chatterjee and Froese, 1975). Experimental studies suggest that there is a solvus between muscovite and paragonite that is asymmetric toward paragonite (i.e., less K in Pg than Na in Mu) and that the solvus does not close due to truncation by other phase assemblages. The form of the solvus between muscovite and paragonite has been used as a geothermometer for metamorphic rocks despite uncertainties resulting from pressure, Ca-Na substitution in paragonite, possible phengite/celadonite solid solutions, and submicroscopic interlayering of mica with other phyllosilicates and of muscovite with paragonite. Moreover, the exact form of the miscibility gap between muscovite and paragonite is still not well constrained (Essene, 1989).

Guidotti (1984) reviewed dioctahedral white mica relations and concluded that the limits of solid solution

* Contribution No. 497 from the Mineralogical Laboratory, Department of Geological Sciences, The University of Michigan, Ann Arbor, Michigan 48109-1063.

in coexisting muscovite and paragonite are generally more restricted than those of micas in single-mica assemblages. He noted that solid solution limits observed in middle-grade metamorphic rocks for muscovite and paragonite correspond approximately to $Mu_{62}Pg_{38}$ and $Mu_{20}Pg_{80}$, respectively. In a study of paragonite and phengite in a blueschist, Shau *et al.* (1991) obtained compositions intermediate to those of phengite and paragonite by microprobe analysis, but those compositions were shown by transmission electron microscopy (TEM) and analytical electron microscopy (AEM) to be due to very fine-scale intergrowths of phengite and paragonite of nearly end-member compositions. Such fine-grained intergrowths of phengite and paragonite were also documented by Ahn *et al.* (1985), further indicating that the relatively wide range of compositions of such phases determined by electron microprobe commonly correspond to mixtures, rather than of single phases with restricted compositions.

The existence of single-phase micas with compositions within the solvus is implied by the reported occurrence of 6:4 regular mixed-layer paragonite : muscovite (or paragonite : phengite) in low-grade anchizonal to epizonal pelitic rocks, based on weak (00*l*) reflections as observed in powder X-ray diffraction (XRD) patterns (e.g., Frey, 1969; Kisch, 1983; Frey, 1987, and references therein). However, such materials have never directly been observed, principally because grains are far too small to be resolved by conventional techniques. Li *et al.* (1992a) and Jiang and Peacor (1993) recently observed a wide variety of intergrown white micas in hydrothermally altered metabasites from North Wales, including homogeneous single-phase Na/K micas with compositions well within the solvus. Because such micas gave XRD patterns identical to those reported for the 6:4 phase, Jiang and Peacor inferred that such ordered phases may not exist. They attributed the existence of one-phase micas of intermediate composition to the nonequilibrium conditions of formation associated with hydrothermal solutions in a contact metamorphic environment. Intergrown packets of discrete muscovite and paragonite with interfaces oblique to 001 were shown to be caused by redistribution of Na and K following formation of homogeneous Na/K mica.

Livi *et al.* (1988) reported similar intergrowths of paragonite and illite (scale $\leq$50 nm) in Alpine black shales, implying the prior existence of metastable micas with compositions within the paragonite-illite solvus, in a prograde metamorphic environment. Based largely on XRD data, Merriman and Roberts (1985) have proposed that Na/K micas progress from random mixed-layer Na/K mica containing up to 15% of randomly interlayered smectite through finely interlayered muscovite and paragonite, to coarse intergrowths of discrete muscovite and paragonite in prograde sequences spanning late diagenesis to the epizone. However, the nature of the earliest phases in such a sequence remains in question, especially in that such prograde conditions normally approach those of equilibrium in contrast to the contact metamorphic conditions for rocks studied by Jiang and Peacor (1993) and because under equilibrium conditions a wide solvus exists.

During characterization of chlorite-mica stacks occurring in an anchizonal mudrock from central Wales (Li *et al.*, 1992b, 1994), white micas with apparent intermediate Na/K compositions were found (Li *et al.*, 1992a). In this sample, forming part of a complete sequence from late diagenesis through the epizone, homogeneous intermediate Na/K micas ranging in composition from $Mu_{86}Pg_{14}$ to $Mu_{58}Pg_{42}$ were observed occurring in the fine-grained matrix. In this paper, we describe the relations that verify that homogeneous, metastable white micas of intermediate compositions can occur early in sequences of prograde metamorphism of pelites and document the transitions to discrete muscovite and paragonite.

PROCEDURE

Specimen

The sample was selected for TEM study from a suite of 663 mudrock samples used for an XRD survey of white mica (illite) crystallinity across the central part of the Lower Paleozoic Welsh Basin (Merriman *et al.*, 1992). It is representative of typical low anchizonal mudrock lithologies, widely developed in central Wales, which are considered to be largely the result of depth-related, very low-grade regional metamorphism (Roberts *et al.*, 1991).

The sample studied is a highly laminated Llandovery mudrock with spaced cleavage from near Rhayader, central Wales. It has a very fine-grained matrix consisting largely of submicroscopic white micas and chlorite. Grains with a modified detrital outline and consisting of subparallel packets of chlorite and white mica, referred to as chlorite-mica stacks, range from 10–150 μm in size and are dispersed throughout the matrix, along with occasional quartz and albite clasts. The occurrence and origin of the chlorite-mica stacks have been studied by many workers (e.g., Craig *et al.*, 1982; Woodland, 1985; Dimberline, 1986; Milodowski and Zalasiewicz, 1991; Li *et al.*, 1992b). Li *et al.* (1994) concluded that they were largely detrital biotite grains, subsequently modified during the progression from diagenesis to low-grade metamorphism. The sample has undergone low-grade metamorphism (lower anchizone) and has a white mica (illite) crystallinity index (half-height peak breadth of the white mica 10 Å peak; Kubler, 1968) of 0.35° $\Delta 2\theta$ (Cu$K\alpha$ radiation).

Methods

XRD data were obtained for the powdered bulk rock sample, using a Philips automated diffractometer with graphite monochromator and Cu$K\alpha$ radiation (35 kV and 15 mA) to define the principal minerals, with quartz as an internal standard. A step size of 0.01° 2θ and a

long counting time of ~5 seconds per step were used to test for overlap of 00*l* reflections of micas. As the d(001) values of micas are strongly dependent on their interlayer composition (Guidotti, 1984), the d ≈ 10.0 Å for muscovite and d ≈ 9.6 Å for paragonite are used to calculate different composition of intermediate sodium potassium micas.

Polished thin sections were prepared with the surface approximately normal to both bedding and cleavage 1) so that the optimum orientation could be obtained for scanning electron microscope (SEM) observations of textural relations and 2) so that the (001) planes of phyllosilicates would be preferentially oriented parallel to the beam for TEM observations. Following optical and SEM observations using back-scattered electron (BSE) imaging and X-ray energy dispersive spectral (EDS) analysis with a Hitachi S-570 scanning electron microscope operated at 15 kV to outline the areas of interest, ion-milled TEM specimens were prepared following the method described by Li *et al.* (1994). TEM observations and AEM analyses were obtained using a Philips CM12 scanning transmission electron microscope (STEM) fitted with a Kevex Quantum solid-state detector and computer system. The STEM was operated at an accelerating voltage of 120 kV and a beam current of ~10 μA to obtain TEM images and SAED patterns. AEM quantitative chemical analyses were obtained using the standards muscovite (K, Al), clinochlore (Mg, Al, Fe), albite (Na, Al), fayalite (Fe), rhodonite (Mn, Fe, Ca), and sphene (Ti, Ca) to derive k-ratios, which were utilized to process EDS data, assuming the thin-foil approximation (Cliff and Lorimer, 1975).

RESULTS

SEM observations and XRD data

The laminated mudrock consists of coarse-grained chlorite-mica stacks, quartz, white mica, chlorite, and a small amount of albite dispersed in a very fine-grained matrix primarily consisting of phyllosilicates. Chlorite-mica stacks are commonly 10–150 μm in size, with (001) planes of intergrown chlorite and white mica parallel or subparallel to each other; the (001) basal planes of most chlorite-mica stacks are in turn oriented parallel or subparallel to bedding. However, chlorite-mica stacks commonly are markedly deformed, with some stacks being cross-cut by ruptures that are parallel to the spaced, pressure-solution cleavage. Such spaced cleavage is approximately 30°–50° to bedding in general, although the orientations may differ by up to 90° in selected areas. Bending and rotation of entire chlorite-mica stacks toward the cleavage are occasionally seen (e.g., Milodowski and Zalasiewicz, 1991; Li *et al.*, 1994).

Phyllosilicates in the matrix are dominantly white mica with subordinate chlorite and constitute a large proportion of the phyllosilicates in the mudrock. In contrast to the grains with detrital-like shapes, they occur as submicroscopic packets of layers that are usually less than 2 μm in size, with their (001) planes principally oriented parallel to one of two preferred orientations. The more abundant type of matrix mica is oriented parallel or subparallel to bedding in the microlithons (S_0, Q-domains), whereas the second, less abundant type is preferentially oriented parallel to cleavage in the relatively thin P-domains (S_1), as seen in SEM images (c.f. Li *et al.*, 1994). However, exceptions occur where (001) of grains of fine-grained matrix mica and chlorite are displaced around detrital grains.

Chlorite (chamosite, as verified by EDS analysis), white mica, quartz, and albite are the principal minerals detected by XRD data. Splitting of the basal reflections of mica is displayed in the XRD pattern (Figure 1), suggesting the presence of more than one mica. The XRD patterns of all micas were indexed on the basis of a 2-layer polytype because the TEM study showed that most of the micas (including white mica in chlorite-mica stacks) in this sample consist of the $2M_1$ polytype (Li *et al.*, 1992a, 1992b, 1994). The strong 002 peak (d = 9.96 Å) has a very weak shoulder with d = 9.60 Å. The 4th-order basal reflections with d = 5.01 Å and d = 4.99 Å also show small shoulders with d = 4.94 Å, d = 4.88 Å, and d = 4.81 Å. The value of 9.96 Å represents a K-rich mica that probably is phengitic muscovite from the chlorite-mica stacks and K-rich mica in the matrix (see below and Li *et al.*, 1994). The weak peaks at d = 9.60 Å and d = 4.81 Å imply a small amount of paragonite, and small peaks at d = 4.94 Å, d = 4.88 Å, and others presumably indicate the presence of micas with compositions ~$Mu_{70}Pg_{30}$, ~$Mu_{58}Pg_{42}$, and other Na/K micas intermediate in composition to muscovite and paragonite. The weaker shoulders at d = 4.94 Å and d = 4.88 Å suggest that the amount of intermediate Na/K mica relative to that of K-rich mica is very small. Similar features were also observed for the 6th-order basal reflections (d ≈ 3.3), although they are overlapped by peaks of other phases to some degree. Similar split reflection features for the basal reflections of intermediate Na/K mica have also been observed for the so-called 6:4 regular mixed-layer paragonite/muscovite in clay separates of low-grade metamorphic pelites by many workers (e.g., Frey, 1969, 1970, 1978; Kisch, 1983; Merriman and Roberts, 1985) and for micas in hydrothermally altered metabasite (Jiang and Peacor, 1993). As we have also concluded here (see below for discussion), such features were inferred by Jiang and Peacor (1993) to reflect the presence of a homogeneous mica of intermediate composition.

TEM observations

TEM images show that, in contrast to the dominance of chlorite in chlorite-mica stacks, white mica is the principal phyllosilicate in the matrix. Lattice fringe im-

https://doi.org/10.1346/CCMN.1994.0420401 Published online by Cambridge University Press

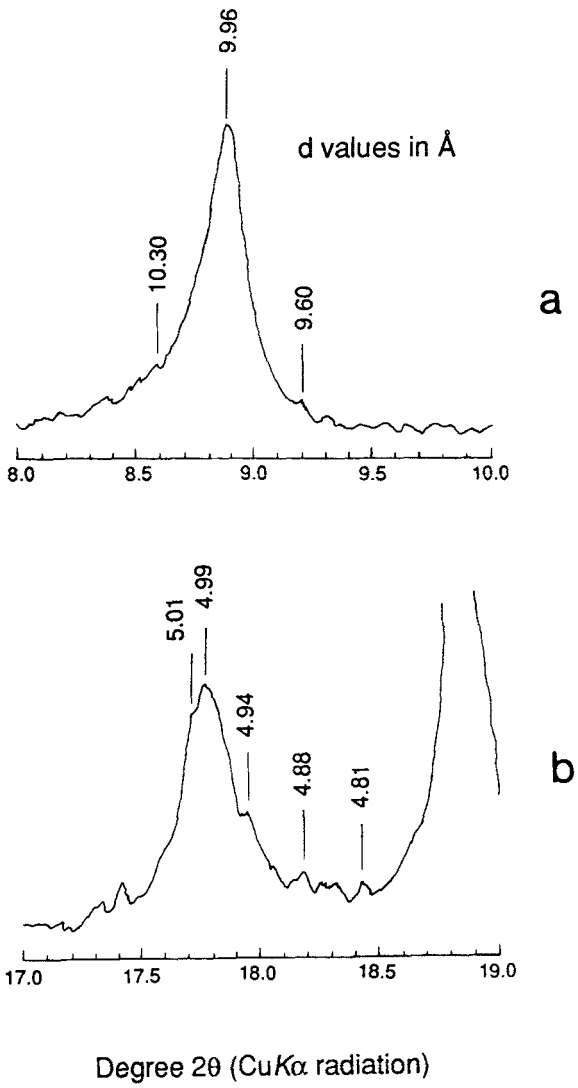

Figure 1. XRD powder diffraction pattern of the bulk rock sample showing (a) the 2nd- and (b) the 4th-order basal reflections of micas.

ages and SAED patterns having (001) reflections of matrix phyllosilicates confirm that in the microlithons, basal planes of matrix white mica and chlorite are broadly bedding-parallel, but that in the narrower P-domains (S_1) basal planes are subparallel to the cleavage direction. At the TEM scale, this relationship may range up to 90° (Figure 2). There is a range of orientations of both bedding- and cleavage-parallel matrix phyllosilicates about the bedding- and cleavage-parallel directions, with subparallel packets of layers displaying a fan-like texture with orientations differing by up to 30°. As was the case for SEM observations, TEM images show that, where large detrital grains occur, the matrix phyllosilicates generally have (001) basal planes oriented parallel to the detrital grain

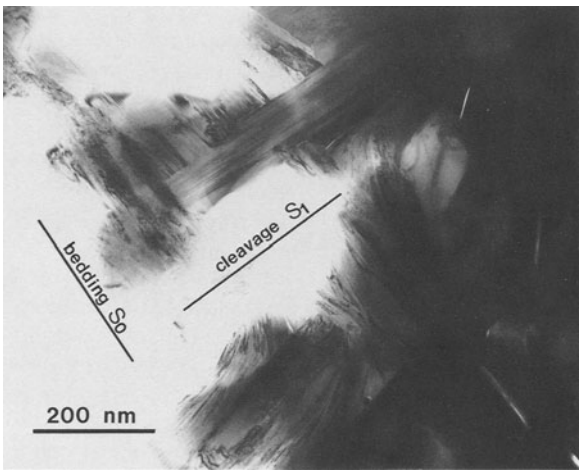

Figure 2. Low magnification TEM image showing two orientations of phyllosilicates in the matrix: one subparallel to sedimentary bedding (S_0, Q-domain) and one subparallel to cleavage (S_1, P-domain), which is, in turn, approximately perpendicular to bedding in this particular image.

boundaries and, therefore, have a wide range of orientations determined by the geometry of the surface of the detrital grains.

Bedding-parallel white mica consists of both very fine-grained deformed crystals (≤200 Å thick) and coarse-grained undeformed crystals (up to 2 μm in thickness). Cleavage-parallel white mica is relatively undeformed (100 Å to 2 μm in thickness) and sometimes occurs as discrete crystals with platy euhedral to subhedral cross-sections (Li *et al.*, 1994).

The smallest crystals of matrix bedding-parallel white mica are generally less than 200 Å in thickness (as thin as 50 Å), occur as subparallel packets with low angle grain boundaries, and contain high concentrations of layer terminations. Kinked, bent, and curved layers are frequently observed, and they are associated with lenticular voids between layers (Figure 3). These strain features show that the small white mica crystals have been subjected to deformation. The inset electron diffraction pattern is typical of such white mica and confirms that it is primarily a disordered $1M_d$ polytype, although some grains consisting of a 2-layer polytype were occasionally seen.

The relatively coarse-grained, subparallel crystals of white mica in the bedding orientation occur as well-defined packets of layers that display little or no deformation and appear to be relatively defect-free in larger range (Figure 4). The lenticular fissures along layers and "mottled" structure are in part due to cation diffusion induced by the electron beam. Relatively coarse-grained white mica displays (00*l*) lattice fringes having contrast with periodicities of around 10 Å and 20 Å, and the inserted SAED pattern (Figure 4) shows that the white mica is a well-crystallized, two-layer

https://doi.org/10.1346/CCMN.1994.0420401 Published online by Cambridge University Press

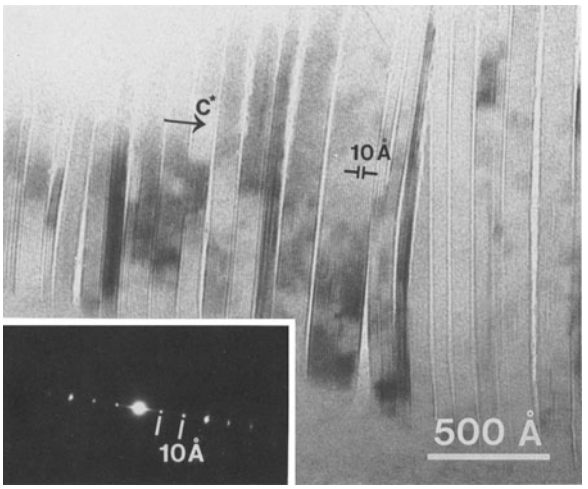

Figure 3. Lattice fringe image of fine-grained white mica in the matrix displaying various defects such as kinking, bending, and layer terminations. The inset electron diffraction pattern of white mica indicates a disordered $1M_d$ polytype, with streaking along c*.

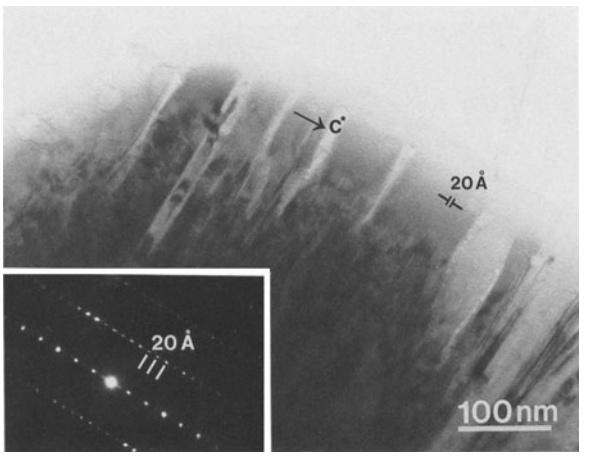

Figure 4. Lattice fringe image of relatively coarse-grained and defect-free matrix white mica. Lenticular splitting along layers is due to beam damage during TEM observation. The inset electron diffraction pattern shows that it is a well-crystallized two-layer polytype ($2M_1$).

polytype (shown to be $2M_1$ by other SAED patterns). Most importantly, only one set of reflections was observed, implying the presence of only one, homogeneous phase. Minor streaking along c* occurred in some SAED patterns of such white mica, where only 00*l* reflections were present, implying some random differences in structure or composition between layers. Only ~10 Å fringes were observed in equivalent lattice fringe images, implying that structure was not a variable, and AEM analyses showed that some micas have compositions with subequal Na and K contents (e.g., Table 1, analysis 3), corresponding to metastable phases. The diffuseness was, therefore, ascribed to some local ordering of Na and K, as consistent with conclusions regarding the modulated structure described below.

Unusual satellite reflections with apparently rational indices were observed in the electron diffraction pattern of one relatively coarse-grained white mica crystal. As shown in Figure 5a, the 00*l* diffraction spots from the single structure are strong, widely spaced, and sharply defined; whereas, the long-period satellite spots are much weaker and more closely spaced. Averaged as ~80 Å, the spacings of these satellite spots are integral multiples of the single structure spacing that is ~20 Å, within error. The superstructure reflections occur in those SAED patterns that contain only 00*l* reflections and, therefore, cannot be caused by polytypism (Peacor, 1992). The reflections, therefore, indicate the presence of a commensurate modulation since the superstructure spots are rational multiples of the

Table 1. Representative structural formulae of matrix white mica.[1]

	Bedding-parallel				Cleavage-parallel		
	1	2	3	4	5	6	7
Si	6.09	6.02	6.03	6.01	6.24	6.05	6.18
Al^{IV}	1.91	1.98	1.97	1.99	1.76	1.95	1.82
Al^{VI}	3.71	3.77	3.91	3.87	3.71	3.92	3.65
Ti	0.02	0.01	0.02	0.02	0.04	0.03	0.05
Fe^{2+}	0.11	0.06	0.07	0.09	0.15	0.05	0.17
Mg	0.16	0.16	n.d.	0.02	0.10	n.d.	0.13
Ca	n.d.	n.d.	n.d.	0.02	n.d.	n.d.	n.d.
Na	0.25	0.52	0.74	1.48	0.43	1.69	n.d.
K	1.56	1.25	1.01	0.17	1.42	0.11	1.82
Total cations	13.81	13.77	13.75	13.67	13.85	13.80	13.82
Na/(K + Na + Ca)	0.14	0.29	0.42	0.89	0.23	0.94	0

[1] Each formula is normalized on the basis of 12 cations on tetrahedral and octahedral sites, and all Fe is calculated as FeO. Two standard deviations on the basis of calculating statistics are 0.11–0.14 pfu for Si, 0.04–0.05 and 0.08–0.09 pfu for Al^{IV} and Al^{VI}, respectively, ≤0.01 pfu for Ti and Ca, 0.01–0.03 pfu for Fe, 0.01–0.02 pfu for Mg, 0.04–0.11 pfu for Na, and 0.06–0.12 pfu for K.

n.d. = not detectable.

https://doi.org/10.1346/CCMN.1994.0420401 Published online by Cambridge University Press

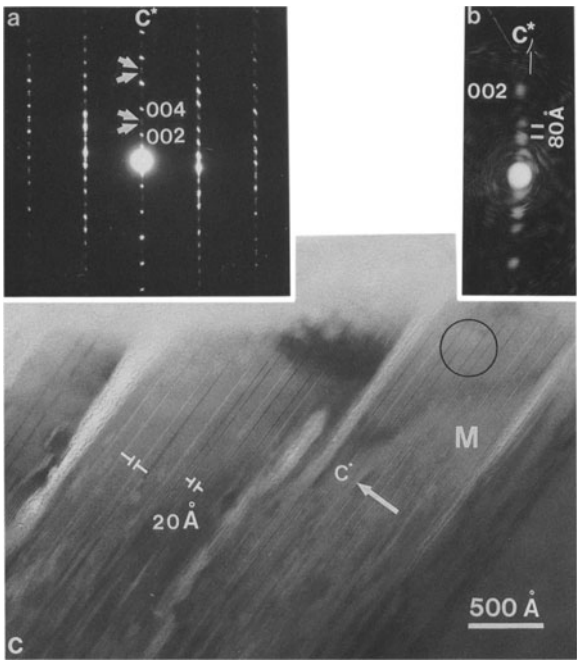

Figure 5. TEM photographs of modulated white mica (M) in the matrix: a) SAED pattern of white mica with a modulated structure having periodicity of approximately 80 Å [the satellite spots (indicated by arrows) are much weaker and more closely spaced than the sharply defined diffraction spots from the substructure]; b) optical diffraction pattern of circled area in Figure 5c showing 80 Å periodicity; and c) lattice fringe image of white mica from which the SAED pattern was obtained, showing two-layer polytypism with 20 Å periodicity [dark and light bands parallel to (001) have spacings of 40 to 120 Å].

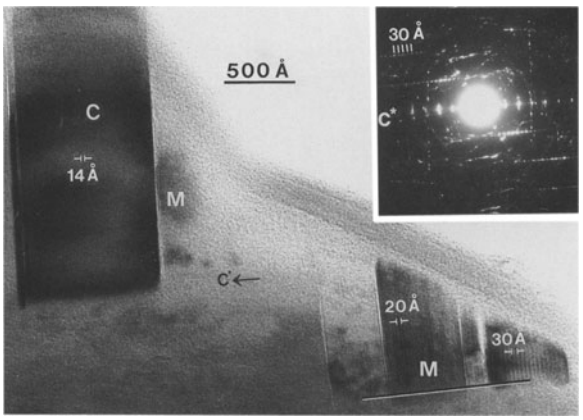

Figure 6. TEM image of cleavage-parallel matrix white mica (M) and chlorite (C). Platy subhedral white mica crystals are 2- and 3-layer polytypes, and platy chlorite displays defect-free fringes with 14 Å periodicity. The inset diffraction pattern of corresponding 3T white mica shows 30 Å periodicity.

substructure (Buseck and Cowley, 1983). A lattice fringe image (Figure 5c) of such white mica, obtained where the corresponding SAED pattern contains non-00*l* reflections, has a "mottled" texture typical of all micas and shows two-layer polytypism with periodicity of 20 Å. Most importantly, there are dark and white bands perpendicular to c* with separations ranging from 40 Å to 120 Å. Optical diffraction patterns of the areas of photographic negatives, with dark and white bands as in Figure 5c, show that the whole area consists of several domains with different periodicities, each corresponding to those of the "bands," e.g., an optical transform of the circled area (which has bands with 80 Å periodicity) gave a diffraction pattern with 80 Å periodicity (Figure 5b). The "bands," therefore, reflect the source of the modulation.

The matrix cleavage-parallel white mica is generally a $2M_1$ polytype and is relatively defect-free, similar to the more coarsely grained matrix white mica in the bedding orientation. Some cleavage-parallel white mica was observed to have a striking texture consisting of platy subhedral individual crystals (100 Å–1000 Å thick) (Figure 6). It consists of straight, defect-free layers that are parallel to crystal boundaries. Although 2-layer polytypes were ubiquitously observed in other crystals, such material consists of both 2- and 3-layer polytypes. These crystal shapes were shown to correspond to cross-sections of platy pseudohexagonal crystals in shales from the Salton Sea geothermal field (Yau *et al.*, 1987b), in Triassic volcanogenic sediments from the Southland Syncline, New Zealand (Ahn *et al.*, 1988), and white mica synthesized under hydrothermal conditions (Yau *et al.*, 1987a), implying that they have crystallized from fluids in the cleavage orientation.

Some SAED patterns of bedding-parallel white mica show split pairs of 00*l* reflections with the splitting distance approximately half of the difference between 00*l* reflections of muscovite and paragonite, suggesting the presence of intermediate Na/K mica. For example, one set of weak (00*l*) diffraction spots (Figure 7a) with ~19.6 Å periodicity was observed in an SAED pattern of white mica, coexisting with a set of strong reflections with ~20.0 Å periodicity. Doubling of (00*l*) spots can be better resolved with the reflections 008 to 0,0,16. The d-values of those reflections correspond to an intermediate Na/K mica ($Mu_{58}P_{42}$) and muscovite, respectively, as consistent with conclusions based on XRD data. Reflections in non-(00*l*) rows indicate that both muscovite and intermediate Na/K mica occur as well-defined two-layer polytypes. The corresponding lattice fringe image shows that the 001 fringes of the intermediate Na/K mica are wavy and distorted as a result of being easily damaged by the electron beam (Figure 7b), in marked contrast to fringes of white micas of near end-member compositions. This was also observed for TEM images of intermediate Na/K micas occurring in hydrothermally altered metabasites (Jiang and Peacor, 1993) and paragonite in blueschist eclogite (Ahn *et al.*, 1985).

https://doi.org/10.1346/CCMN.1994.0420401 Published online by Cambridge University Press

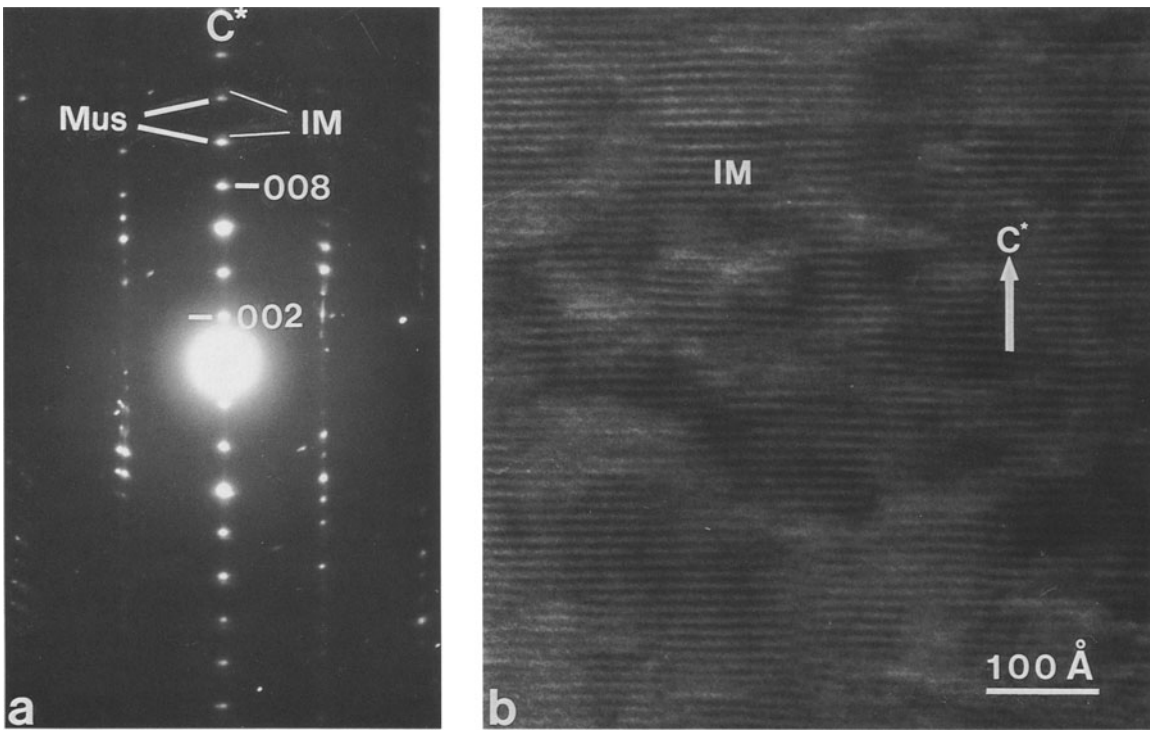

Figure 7. TEM images of coexisting muscovite (Mus) and intermediate Na/K mica (IM): a) SAED pattern of matrix, bedding-parallel muscovite and intermediate Na/K mica [weak (00*l*) reflections of intermediate Na/K mica with 19.6 Å periodicity may be resolved from stronger ones of 20 Å for muscovite from the reflections (008) to (0,0,16)]; and b) lattice fringe image of corresponding intermediate Na/K mica (the layers are wavy and not as straight as those for white mica in other photographs).

The SAED patterns of cleavage-parallel white mica commonly display split pairs of 00*l* reflections with 20 Å and 19.2 Å periodicity, corresponding to discrete muscovite and paragonite, respectively (Figure 8). Such splitting was only rarely observed in SAED patterns of bedding-parallel white mica. The discrete muscovite and paragonite are both 2-layer polytypes; in those cases where the specific polytype was identified, it was $2M_1$. Both the interfaces between muscovite and intermediate Na/K mica, and between muscovite and paragonite were observed to be parallel to the basal planes. All cleavage-parallel phyllosilicates, including chlorite, occurred as discrete packets of layers; no mixed-layering of white micas or of white mica and chlorite was observed.

AEM analysis

The compositions of many (>200) grains of matrix bedding-parallel and cleavage-parallel white mica were determined, only from areas demonstrated by TEM to be single phases. Representative compositions of typical bedding-parallel and cleavage-parallel matrix white micas are given in Table 1. All white micas have compositions approaching those of ideal micas, with net negative charges of nearly 2.0. Such compositions correspond to evolved micas rather than to authigenic illite for which net negative charges are considerably smaller (~1.6, Środoń *et al.*, 1986; Jiang *et al.*, 1992).

The compositions [Na/(Na + K + Ca) ~ 0.14–0.42] of most bedding-parallel white mica (analyses 1–3) and some cleavage-parallel white mica (e.g., analysis 5) are incompatible with the wide solvus in the system muscovite-paragonite (e.g., Eugster, 1956; Eugster *et al.*, 1972; Blencoe and Luth, 1973). Attempts to determine the spatial distribution of Na and K were, therefore, made in order to determine if the intermediate compositions were caused by overlap of the beam on more than one mica. More than twenty AEM analyses were, therefore, obtained using a stationary electron beam in STEM mode with 50 Å beam diameter for areas shown by SAED to consist only of a single phase. Those results verified the presence of intermediate compositions in all of the fine-grained deformed bedding-parallel white mica (e.g., analysis 3). The analyses with Na/(Na + K + Ca) ~ 0.42 corresponding to $Mu_{58}Pg_{42}$ are consistent with compositions as determined both by XRD and SAED patterns.

The relatively coarse-grained and defect-free bedding-parallel white mica displays either intermediate compositions with smaller Na/(Na + K + Ca) ratios (analysis 2) than those of fine-grained white mica or compositions of discrete near-endmember muscovite

https://doi.org/10.1346/CCMN.1994.0420401 Published online by Cambridge University Press

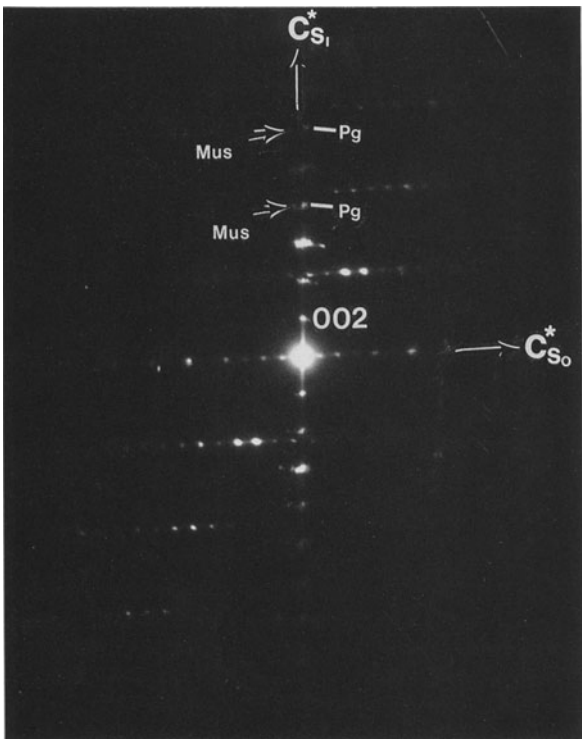

Figure 8. SAED pattern typical of both bedding- and cleavage-parallel white mica. Split pairs of 00*l* reflections of muscovite (with 20 Å periodicity) and paragonite (with 19.2 Å periodicity) are displayed in cleavage-parallel white mica. All white micas are two-layer polytypes.

($Mu_{93}Pg_7$) and paragonite ($Mu_{11}Pg_{89}$, analysis 4). Analysis 2, having a relatively high Na content [Na/(Na + K + Ca) ~ 0.29], corresponds to the bedding-parallel white mica with commensurate modulated structure.

The cleavage-parallel white micas generally have compositions approaching those of endmember muscovite [e.g., Na/(Na + K + Ca) = 0, analysis 7] and paragonite [e.g., Na/(Na + K + Ca) = 0.94, analysis 6], although some white mica has significant Na (e.g., analysis 5).

Bedding-parallel white mica in the matrix has Fe + Mg contents of 0.07–0.27 per formula unit (pfu), Ti contents of 0.01–0.02 pfu. A small amount of Ca (0.02 pfu, e.g., analysis 4) was detected in some bedding-parallel mica. In contrast, white mica (except the paragonite, analysis 6) in the cleavage orientation has higher Fe + Mg (0.25–0.30) and Ti (0.03–0.05) content. With respect only to cleavage-parallel mica, the Fe and Mg contents of muscovite are clearly greater than those of paragonite. No Ca was detected in cleavage-parallel white mica. In further contrast with white mica parallel to bedding, cleavage-parallel mica has a smaller deficiency of total interlayer cations (1.80–1.85 pfu), as consistent with a greater degree of evolution toward ideal mica.

DISCUSSION

Status of 6:4 mixed-layer mica

The existence of Na/K mica with compositions within the limbs of the solvus has also been implied by reports of 6:4 ordered mixed-layer paragonite/muscovite (Frey, 1969, 1970, 1987; Kisch, 1983; Merriman and Roberts, 1985; Roberts *et al.*, 1991). In most cases, identification was based on weak and poorly defined peaks in X-ray diffraction patterns that did not include any superstructure reflections. However, Li *et al.* (1992a) and Jiang and Peacor (1993) have correlated TEM/AEM observations of homogeneous, disordered Na/K mica having compositions within the solvus with XRD data for the same material. They showed that the XRD data observed for the hypothetical 6:4 phase are identical to those of the disordered mica occurring in a hydrothermally altered metabasite. They concluded that previous reports of the 6:4 mixed-layer micas actually refer to disordered mica of intermediate composition, implying that the so-called 6:4 phase identified in low-grade sediments may also be a homogeneous, metastable Na/K mica; such is the case in the sample of this study. Disordered, metastable mica may actually be more common in lower grade rocks than heretofore recognized.

Metastability and modulated structure of Na/K mica

The binary solvus between muscovite and paragonite has been studied by many workers using experimental data and data for natural paragonite-muscovite pairs (cf., Guidotti, 1984, and references therein). Muscovite with significant paragonite solid solution was only observed in single-mica assemblages in middle-grade metamorphic rocks, for which the highest Na/(Na + K) ratio observed is ~0.38 (Guidotti, 1984). Such material should be studied by TEM to determine if it is single phase, but even if it is, the Na/(Na + K) ratio is still less than that (0.42) of some Na/K mica in the sample of this study. Shau *et al.* (1991) studied solvus relations of submicroscopically intergrown paragonite and phengite in a blueschist and constrained the phengite-paragonite solvus to values of Na/(Na + K) = <0.02 and 0.97 at T = <200°C and P < 7.4 kb. The compositions of intermediate white micas in the Welsh mudrock fall well within those solvus limits. They are, therefore, metastable, as also consistent with textural data summarized below. Their formation in a prograde (burial) environment must take place only during initial low-temperature stages of diagenesis/metamorphism and, with increasing grade of metamorphism, they should evolve to discrete paragonite and muscovite. The sequence of formation of white micas is discussed in detail below, in the light of such relations.

Although most metastable bedding-parallel mica of intermediate composition shows no superstructure re-

flections, the single grain that displayed unusual satellite reflections is apparently unique among micas. The superperiodicity of ~80 Å (i.e., four times that of the substructure) implies the existence of a commensurate modulated structure, defined as a long-range modulation with periodicity that is a multiple of that of the substructure. The modulation may be caused by either structural distortions or compositional changes or both (Buseck and Cowley, 1983). The modulated structure may, therefore, represent an intermediate state that formed during the process of transformation from one structure to another or during the unmixing of one phase into two or more phases (Morimoto, 1978).

Since paragonite and muscovite are isostructural 2-layer polytypes, the modulation must be primarily caused by composition. The only differences in structure are the result of small shifts in atom positions, which are in turn a function of composition. The modulated white mica has an intermediate composition ($Mu_{71}Pg_{29}$) falling within the solvus. Using the phengite-paragonite solid solution limits constrained by Shau *et al.* (1991), such a composition can be calculated as corresponding to about 25% paragonite and 75% phengitic muscovite, corresponding to two layers (20 Å thick) of paragonite and 6 layers (60 Å thick) of phengitic muscovite. This is consistent with the ~80 Å periodicity obtained by both SAED pattern and optical diffraction pattern, suggesting that the dark and white bands in the lattice fringe images are the result of modulation related to composition. We, therefore, tentatively infer that the modulation is caused by ordering of interlayer K and Na into separate layers. Such ordering may occur through either of two mechanisms: 1) diffusion of Na and K within the phyllosilicate framework, which occurs much more readily along layers than across layers (Veblen 1983); and 2) dissolution of disordered Na/K mica and crystallization of partially ordered metastable mica. The latter mechanism is consistent with the $2M_1$ polytypism of the modulated structure, which may have evolved from bedding-parallel $1M_d$ mica, as described below.

Evolution of micas from diagenesis through low-grade metamorphism

Textural data show that matrix phyllosilicates are preferentially oriented in two directions, one parallel or subparallel to sedimentary bedding and one parallel or subparallel to spaced cleavage. Matrix white micas are intergrown with subordinate chlorite, with individual packets of layers ranging from 50 Å to 2 μm in thickness. Although white mica is homogeneous in both structure and composition within individual grains, the Na/(Na + K) ratios of individual matrix mica grains vary widely. The small (thicknesses <200 Å), deformed (kinked, bent, and with edge dislocations) crystals of bedding-parallel white mica are generally single-phase intermediate Na/K mica with low (Fe + Mg) contents. Larger, strain-free bedding-parallel micas are usually intermediate Na/K mica with less Na content and/or discrete paragonite and muscovite. By contrast, the cleavage-parallel white mica is generally phengitic muscovite (with higher Fe + Mg contents) and discrete paragonite. Bedding-parallel mica of intermediate composition usually occurs as $1M_d$ polytype, whereas the discrete paragonite and muscovite in both bedding- and cleavage-parallel orientations usually occurs as $2M_1$ polytype. The heterogeneity in packet sizes, composition, and polytypism clearly reflect a lack of textural and chemical equilibrium, whereas the presence of intermediate Na/K ratios demonstrates metastability.

The compositional and textural data collectively suggest that white micas have evolved through a sequence of transformations, compatible with Ostwald-step-rule relations wherein processes proceed through steps of successively lower free energy, with specific metastable states occurring as a consequence of the specific reaction paths. Three different stages are recognized: 1) transformation of primary matrix clays, assumed to be largely smectite, to bedding-parallel, fine-grained white mica of intermediate composition during burial diagenesis of the sedimentary sequence; 2) dissolution of strained, fine-grained mica and crystallization of discrete paragonite and muscovite in the bedding-parallel orientation, following deep burial of the sequence; and 3) dissolution of bedding-parallel white micas, and crystallization of discrete muscovite and paragonite in the cleavage-parallel orientation during basin inversion and deformation. Each of these proposed stages is separately discussed below.

The earliest transformation recognized is the formation of homogeneous, metastable Na/K mica. The formation of illite, in which K is the dominant interlayer cation, through reactions involving detrital smectite in a burial diagenetic environment is well established (e.g., see review in Freed and Peacor, 1992). Similarly, a number of authors have suggested that Na-rich equivalents of illite may be derived through reactions in which primary smectite plays a central role (Frey, 1969, 1970; Merriman and Roberts, 1985; Livi *et al.*, 1988; Shau *et al.*, 1991). The TEM/AEM characteristics of some bedding-parallel Na/K micas are typical of clay minerals that formed at the earliest stages of prograde sequences of pelites, as reviewed by Peacor (1992). These include the following:

1) Crystal size. Packets a few tens of angstroms in thickness are typical of clay minerals that have transformed from smectite at the lowest grades of diagenesis and that have not been further modified. The thickness of early-formed packets of white micas increases with increasing grade (e.g., Merriman *et al.*, 1990).
2) Metastability of phases. The occurrence of metastable micas with compositions within the solvus

is typical of formation at low temperature, where sluggish rates of diffusion lead to non-stable equilibrium relations.

3) Heterogeneity of composition. Although individual packets of bedding-parallel micas were observed to be relatively homogeneous in composition, adjacent packets varied widely in composition, a fundamental condition for chemical non-equilibrium.
4) Crystal defects. The smallest crystals were observed to have high concentrations of layer terminations and commonly show stacking disorder as represented by $1M_d$ polytypism, a feature Grubb *et al.* (1991) noted as typical of illite in its original state as a transformation product of primary smectite. Lee *et al.* (1984, 1986) also noted that early formed illite has higher concentrations of defects, whereas Livi *et al.* (1988) observed that poorly crystalline illite generally has greater concentrations of interlayer vacancies and Na than better-crystallized grains.

The textural and compositional relations, therefore, are collectively consistent with derivation of the metastable, bedding-parallel matrix white mica through dissolution of detrital smectite and crystallization of primary illite. Coexisting chlorite may have formed at the same time as a by-product of the reaction (Perry and Hower, 1970; Hower *et al.*, 1976). TEM observations by Ahn and Peacor (1985, 1989) of illite+chlorite textural relations in Gulf Coast shales are similar to mica+chlorite relations observed in this study and imply that chlorite may have formed as a result of the larger Fe and Mg contents of reactant smectite as compared to product illite.

Variation in the proportions of Na and K in white micas derived through reactions involving smectite appears to be determined by one of two relations: 1) the compositions of the primary matrix clays and volcanogenic materials controlled the interlayer cation content of smectite during transformation of smectite to micas, or 2) crystallization of other Na- or K-rich phases such as feldspars or zeolites controlled the Na/K budget.

Several recent studies have shown, contrary to the commonly held belief that Ca and Na are the dominant cations in smectite interlayers, that K is the dominant cation in smectite of marine shales (Buatier *et al.*, 1992; Freed and Peacor, 1992; Masuda *et al.*, 1992, and personal communication). Although K-rich micas are thought to be the dominant product of authigenesis of smectite because of easier fixation of K^+ relative to Na^+ in illite layers during burial diagenesis even in a Na-rich pore fluid (Eberl, 1980; Środoń and Eberl, 1984), Na-micas are common as major phases coexisting with K-micas in low-grade rocks (e.g., Frey, 1969, 1970, 1978, 1987; Kisch, 1983; Merriman and Roberts, 1985). Merriman and Roberts (1985) found that most pelitic rocks in north Wales contain mixed-layer paragonite-muscovite and/or discrete paragonite and that albite is significantly more plentiful in slate samples containing no paragonite, implying that reactions in which albite is formed are probably a major cause for higher grade rocks (e.g., greenschist facies) being dominated by muscovite, with paragonite being less common. Na-rich clay minerals are, therefore, common products of diagenesis, even though smectite and illite preferentially accept K as the interlayer cation. They must, therefore, derive their Na either through unusually high Na contents of the pore fluids that mediate dissolution of smectite and crystallization of illite or through unusually high Na contents of precursor smectite. Because there is no evidence of unusually saline conditions in the Lower Paleozoic Welsh Basin, the latter is unlikely. However, because interlayer cations of smectite are readily exchanged even at low temperatures, hypothetical pore fluids in contact with precursor smectite in the latter case must also have been transiently Na rich.

It is also likely that the Na/K ratio of white micas transformed from smectite was controlled by formation of other Na- or K-rich phases such as feldspar or zeolite during diagenesis and very low-grade metamorphism. For example, Altaner and Grim (1990) reported the absence of illite in diagenetically altered rhyolitic tuff in the Sucher Creek Formation in eastern Oregon, due to the formation of K-rich clinoptilolite that formed in response to higher activities of K and H_4SiO_4 in the pore fluid than in shale. Masuda *et al.* (1992) studied formation of authigenic smectite and zeolite during early diagenesis of volcanic ash in ocean sediments and found that smectite is initially K-rich with depth, becoming more Na-rich at the greater depth where clinoptilolite forms. On the other hand, as clinoptilolite becomes increasingly K-rich with depth, the formation of illite is inhibited as a result of clinoptilolite's behaving as a sink for K. Such a reaction mechanism is analogous to the suppression of paragonite in favour of albite formation at higher grades. It is, therefore, possible that the high Na/K ratios of some white mica was inherited from smectite that was Na-rich as a result of reactions involving zeolites.

Formation of bedding-parallel discrete muscovite and paragonite represents the second stage of the proposed sequence of phyllosilicate transformations recognized here. Some muscovite and paragonite in the bedding-parallel orientation have characteristics that are more evolved than those formed by the initial smectite to illite transformation. These include: 1) relatively large crystal size, with packet thicknesses up to 2 μm; 2) low concentrations of defects such as layer terminations; 3) occurrence of $2M_1$ and lack of $1M_d$ polytypes; 4) compositions approaching those of the approximate solvus limits; and 5) compositions approaching those of mature micas, with net negative charges of nearly

2.0. Such properties are characteristic of 2:1 phyllosilicates that have evolved beyond the initial states of transformation from smectite.

It is commonly observed that phyllosilicates crystallize with (001) normal to the maximum principal stress direction. However, when illite forms in response to deep burial it is subject only to isotropic lithostatic pressure, but mimetic crystallization tends to emphasize any original depositional or compositional fabric. In central Wales, at least 5.5 km of stratigraphic overburden is inferred to have accumulated prior to basin inversion and deformation (British Geological Survey, 1993). Detailed surveys of white mica (illite) crystallinity across the Welsh Basin suggest that, combined with a higher than normal field gradient, the thickness of overburden was sufficient to produce a depth-related pattern of metamorphism (Roberts *et al.,* 1991; Merriman *et al.,* 1992). The formation of discrete paragonite and muscovite in the bedding-parallel orientation is, therefore, consistent with crystal growth during burial metamorphism. This is the first evidence for such a transition, forming a bridge between the diagenetic environment in which smectite or metastable illite are the common clay minerals and the low grade metamorphic environment dominated by tectonically induced cleavage formation and the growth of mature micas.

The final stage in the proposed sequence of transformation is the formation of cleavage-parallel muscovite and paragonite. White micas with orientations parallel to slaty cleavage are relatively mature micas with the following characteristics: 1) crystals are relatively large with packet thicknesses up to 2 μm; 2) as shown in Figure 6, some packets have subhedral cross-sections that resemble cross sections of euhedral pseudohexagonal crystals that crystallized from hydrothermal fluids (Yau *et al.,* 1987a, 1987b); 3) the compositions of crystals approach those corresponding to the solvus limits (e.g., $Mu_{100}Pg_0$ and Mu_6Pg_{94}), with a relatively narrow range of compositions; and 4) all crystals for which a full set of observations has been made consist of the stable $2M_1$ or 3T polytypes. These characteristics collectively imply that the cleavage-parallel paragonite and muscovite are the most evolved micas formed through dissolution of pre-existing micas and crystallization in the cleavage-parallel orientation.

In general, cleavage-parallel white micas have compositions intermediate to those of bedding-parallel white mica and white mica in coarse chlorite-mica stacks. They are similar to the former in having relatively high Na/(Na + K + Ca) ratios and to the latter in high Si/Al and Fe/(Fe + Mg) ratios, and Fe and Mg contents (Li *et al.,* 1994). Similarly, cleavage-parallel chlorite also has a composition intermediate to that in the bedding-parallel orientation (lower Fe content) and that in stacks (higher Fe content). These data further imply that cleavage-parallel chlorite and white mica formed by dissolution of bedding-parallel phyllosilicates and chlorite-mica stacks. Cleavage development can be related to the inversion of the Welsh Basin, with resulting deformation of the sedimentary sequence during the Acadian (late Lower Devonian) phase of tectonics.

Ohr *et al.* (1994) have obtained Sm-Nd ages for the fine-grained clay fraction of rocks from the same prograde assemblage that provided the specimen described in this study. For uncleaved specimens from the zone of diagenesis, the ages correspond approximately to the time of sedimentation to early diagenesis. Ages of anchizonal samples with slaty cleavage give ages intermediate to the ages of diagenesis and metamorphism. Those results are consistent with the observations of this study, in that samples from diagenetic zone have only a bedding-parallel, burial-metamorphic-derived, matrix component, whereas those of increasing grade within the anchizone have an increasing proportion of cleavage-parallel, metamorphic mica; the variable ages of samples with both bedding- and cleavage-parallel components are, thus, weighted averages of the separate, specific diagenetic and metamorphic ages.

ACKNOWLEDGMENTS

We thank Y.-H. Shau and W.-T. Jiang for helpful discussions and C. Henderson for maintaining the instruments of the University of Michigan Electron Microbeam Analysis Laboratory. We also acknowledge Drs. R. E. Ferrell Jr. and G. R. Thompson for their critical and constructive reviews. This work is supported by NSF grants EAR-88-17080 and EAR-91-04565 to D. R. Peacor. The STEM used in this study was acquired under grant EAR-87-08276, the SEM under grant BSR-83-14092, and the microprobe under grant EAR-82-12764 from the National Science Foundation. R. J. Merriman publishes by permission of the director, British Geological Survey (N.E.R.C.).

REFERENCES

Ahn, J. H. and Peacor, D. R. (1985) Transmission electron microscopic study of diagenetic chlorite in Gulf Coast Argillaceous sediments: *Clays & Clay Minerals* **33,** 228–236.

Ahn, J. H. and Peacor, D. R. (1989) Illite/smectite from Gulf Coast shales: A reappraisal of transmission electron microscope images: *Clays & Clay Minerals* **37,** 542–546.

Ahn, J. H., Peacor, D. R., and Coombs, D. S. (1988) Formation mechanisms of illite, chlorite and mixed layer illite-chlorite in Triassic volcanogenic sediments from the Southland Syncline, New Zealand: *Contrib. Mineral. Petrol.* **99,** 82–89.

Ahn, J. H., Peacor, D. R., and Essene, E. J. (1985) Coexisting paragonite-phengite in blueschist eclogite: A TEM study: *Amer. Mineral.* **70,** 1193–1204.

Altaner, S. P. and Grim, R. E. (1990) Mineralogy, chemistry, and diagenesis of tuffs in the Sucher Creek Formation (Miocene), eastern Oregon: *Clays & Clay Minerals* **38,** 561–572.

Bayliss, S. W. (1975) Nomenclature of the trioctahedral chlorites: *Can. Mineral.* **13,** 178–180.

Blencoe, J. G. (1974) An experimental study of muscovite-

paragonite stability relations: Ph.D. dissertation, Stanford University, Palo Alto, California.

Blencoe, J. G. and Luth, W. C. (1973) Muscovite-paragonite solvi at 2.4 and 8 kb pressure: *Geol. Soc. Amer. Abstr. Programs* **5,** 553–554.

British Geological Survey (1993) *Rhayaden.* England & Wales Sheet 179. Solid. (1:50,000: Southampton: Ordnance Survey for British Geological Survey).

Buatier, M., Peacor, D. R., and O'Neil, J. R. (1992) Smectite-illite transition in Barbados accretionary wedge sediments: TEM and AEM evidence for dissolution/crystallization at low temperature: *Clays & Clay Minerals* **40,** 65–80.

Buseck, P. R. and Cowley, J. M. (1983) Modulated and intergrowth structures in minerals and electron microscope methods for their study: *Amer. Mineral.* **68,** 18–40.

Chatterjee, N. D. and Froese, E. (1975) A thermodynamic study of the pseudobinary join muscovite-paragonite in the system $KAlSi_3O_8$-$NaAlSi_3O_8$-Al_2O_3-SiO_2-H_2O: *Amer. Mineral.* **60,** 985–993.

Cliff, G. and Lorimer, G. W. (1975) The quantitative analysis of thin specimens: *J. Microscopy* **103,** 203–207.

Craig, J., Fitches, W. R., and Maltman, A. J. (1982) Chlorite-mica stacks in low strain rocks from central Wales: *Geol. Mag.* **119,** 243–256.

Dimberline, A. J. (1986) Electron microscope and electron microprobe analysis of chlorite-mica stacks in the Wenlock turbidites, mid Wales, U.K.: *Geol. Mag.* **123,** 299–306.

Eberl, D. (1980) Alkali cation selectivity and fixation by clay minerals: *Clays & Clay Minerals* **28,** 161–172.

Essene, E. J. (1989) The current status of thermobarometry in metamorphic rocks: in *Evolution of Metamorphic Belts,* J. S. Daly, R. A. Cliff, and B. W. D. Yardley, eds., Geological Society Special Publication No. **43,** 1–44.

Eugster, H. P. (1956) Muscovite-paragonite join and its use as a geological thermometer: *Bull. Geol. Soc. Amer.* **67,** p. 1693.

Eugster, H. P., Albee, A. L., Beace, A. E., Thompson Jr., J. B., and Waldbaum, D. R. (1972) The two phase region and excess mixing properties of paragonite-muscovite crystalline solutions: *J. Petrol.* **13,** 147–179.

Freed, R. L. and Peacor, D. R. (1992) Diagenesis and the formation of authigenic illite-rich I/S crystals in Gulf Coast shales: TEM study of clay separates: *J. Sedimen. Petrol.* **62,** 220–234.

Frey, M. (1969) A mixed-layer paragonite/phengite of low-grade metamorphic origin: *Contrib. Miner. Petrol.* **24,** 63–65.

Frey, M. (1970) The steps from diagenesis to metamorphism in pelitic rocks during Alpine orogenesis: *Sediment.* **15,** 261–279.

Frey, M. (1978) Progressive low-grade metamorphism of a black shale formation, central Swiss Alps, with special reference to pyrophyllite and margarite bearing assemblages: *J. Petrol.* **19,** 95–135.

Frey, M. (1987) Very low-grade metamorphism of clastic sedimentary rocks: in *Low Temperature Metamorphism,* M. Frey, ed., Chapman and Hall, New York, 9–58.

Fujii, T. (1966) Muscovite-paragonite equilibria: Ph.D. dissertation, Harvard University, Cambridge, Massachusetts.

Grubb, S. M. B., Peacor, D. R., and Jiang, W.-T. (1991) Transmission electron microscopy observations of illite polytypism: *Clays & Clay Minerals* **39,** 540–550.

Guidotti, C. V. (1984) Micas in metamorphic rocks: in *Micas,* S. W. Bailey, ed., Mineralogical Society of America, Reviews in Mineralogy **13,** 357–467.

Hower, J., Eslinger, E. V., Hower, M. E., and Perry, E. A. (1976) Mechanism of burial metamorphism of argillaceous sediments: 1. Mineralogical and chemical evidence: *Bull. Geol. Sci. Amer.* **87,** 725–737.

Jiang, W.-T., Essene, E. J., and Peacor, D. R. (1990) Transmission electron microscopic study of coexisting pyrophyllite and muscovite: Direct evidence for the metastability of illite: *Clays & Clay Minerals* **38,** 225–240.

Jiang, W.-T., Niet Garcia, F., and Peacor, D. R. (1992) Composition of diagenetic illite as defined by analytical electron microscope analyses: Implications for smectite-illite-muscovite transition: *29th International Geological Congress Abstracts,* Kyoto, Japan, p. 100.

Jiang, W.-T. and Peacor, D. R. (1993) Formation and modification of metastable intermediate sodium potassium mica, paragonite, and muscovite in hydrothermally altered metabasites from northern Wales: *Amer. Mineral.* **78,** 782–793.

Kisch, H. J. (1983) Mineralogy and petrology of burial diagenesis (burial metamorphism) and incipient metamorphism in clastic rocks: in *Diagenesis in Sediments and Sedimentary Rocks,* G. Larsen and G. V. Chilingar, eds., Elsevier, New York, 289–493.

Kreutzberger, M. E. and Peacor, D. R. (1988) Behavior of illite and chlorite during pressure solution of shaly limestone of the Kalkberg Formation, Catskill, New York: *J. Struct. Geol.* **10,** 803–811.

Kubler, B. (1968) Evaluation quantitative du metamorphisme par la cristallinite de l'illite: *Bull. Centre Rech. Pau. SNPA* **2,** 385–397.

Lee, J. H., Peacor, D. R., Lewis, D. D., and Wintsch, R. P. (1984) Chlorite-illite/muscovite interlayered and interstratified crystals: A TEM/STEM study: *Contrib. Mineral. Petrol.* **88,** 372–385.

Lee, J. H., Peacor, D. R., Lewis, D. D., and Wintsch, R. P. (1986) Evidence for syntectonic crystallization for the mudstone to slate transition at Lehigh Gap, Pennsylvania, U.S.A.: *J. Struct. Geol.* **8,** 767–780.

Li, G., Jiang, W.-T., and Peacor, D. R. (1992a) Metastable intermediate Na/K micas in hydrothermally altered metabasites and metamorphosed pelites from Wales: *Geological Society of America Abstracts with Programs* **31,** p. A72.

Li, G., Peacor, D. R., Merriman, R. J., and Roberts, B. (1992b) TEM and AEM study of chlorite-mica stacks in slates, central Wales, U.K.: *29th International Geological Congress Abstracts,* Kyoto, Japan, p. 100.

Li, G., Peacor, D. R., Merriman, R. J., Roberts, B., and Pluijm, B. A. (1994) TEM and AEM constraints on the origin and significance of chlorite-mica stacks in slates: an example from central Wales, U.K.: *J. Struct. Geol.* (in press).

Livi, K. J. T., Veblen, D. R., and Ferry, J. M. (1988) Electron microscope study of anchizone and epizone metamorphosed shales from the central Swiss Alps: *Geological Society of America Abstracts with Programs* **20,** A244.

Livi, K. J. T., Veblen, D. R., and Ferry, J. M. (1990) Segregation of K- and Na-rich micas in low-grade metamorphosed shale from the Liassic Black Shale, Switzerland. International Correlation Programme, Project 294: Very Low Grade Metamorphism, Conference on Phyllosilicates as Indicators of Very Low Grade Metamorphism and Diagenesis, Programme and Abstracts. Manchester, UK, July 4–6, 1990.

Masuda, H., Tanaka, H., Gamo, T., O'Neil, J. R., Peacor, D. R., and Jiang, W-T. (1992) Formation of authigenic smectite and zeolite and associated major element behavior during early diagenesis of volcanic ash in the Nankai Trough, Japan, ODP leg 131: In *Proceedings of 7th International Symposium on Water-Rock Interaction,* Balkema, Rotterdam, 1659–1662.

Merriman, R. J. and Roberts, B. (1985) A survey of white mica crystallinity and polytypes in pelitic rocks of Snowdonia and Llyn, North Wales: *Mineral. Mag.* **49,** 305–319.

Merriman, R. J., Roberts, B., and Hirons, S. R. (1992) Regional low grade metamorphism in the central part of the

Lower Paleozoic Welsh Basin: An account of the Llanilar and Rhayader districts, BGS 1:50k sheets 178 & 179: *British Geological Survey Technical Report* **WG/92/16.**

Merriman, R. J., Roberts, B., and Peacor, D. R. (1990) A transmission electron microscope study of white mica crystallite size distribution in the mudstone to slate transitional sequence, North Wales, UK: *Contrib. Mineral. Petrol.* **106,** 27–40.

Milodowski, A. E. and Zalasiewicz, J. A. (1991) The origin and sedimentary, diagenetic and metamorphic evolution of chlorite-mica stacks in Llandovery sediments of central Wales, U.K. *Geol. Mag.* **128,** 263–278.

Morimoto, N. (1978) Incommensurate superstructures in transformation of minerals: *Recent Progress of Natural Sciences in Japan* **3,** 183–206.

Ohr, M., Halliday, A. N., and Peacor, D. R. (1994) Mobility and fractionation of rare earth elements in argillaceous sediments: Implications for dating diagenesis and low-grade metamorphism: *Geochim. et Cosmochim. Acta.* **58,** 289–312.

Peacor, D. R. (1992) Diagenesis and low-grade metamorphism of shales and slates: in *Minerals and Reactions at the Atomic Scale: Transmission Electron Microscopy,* P. R. Buseck, ed., Mineralogical Society of America, Reviews in Mineralogy **27,** 335–380.

Pe-Piper, G. (1985) Dioctahedral micas in Triassic metavolcanic rocks of western Greece: *Can. Mineral.* **23,** 597–608.

Perry, E. and Hower, J. (1970) Burial diagenesis in Gulf Coast pelitic sediments: *Clays & Clay Minerals* **18,** 165–177.

Popov, A. A. (1968) Composition of muscovites and paragonites synthesized at temperatures of 350°C to 500°C: *Geokhimiya* **2,** 131–144.

Roberts, B., Merriman, R. J., and Pratt, W. (1991) The influence of strain, lithology and stratigraphical depth on white mica (illite) crystallinity in mudrocks from the vicinity of the Corris Slate Belt, Wales: Implications for the timing of metamorphism in the Welsh Basin: *Geol. Mag.* **128,** 633–645.

Rosenfeld, J. R., Thompson Jr., J. B., and Zen, E-an (1958) Data on coexistent muscovite and paragonite: *Geol. Soc. Amer. Bulletin* **69,** 1637.

Shau, Y.-H., Feather, M. E., Essene, E. J., and Peacor, D. R. (1991) Genesis and solvus relations of submicroscopically intergrown paragonite and phengite in a blueschist from northern California: *Contrib. Mineral. Petrol.* **106,** 367–378.

Środoń, J. and Eberl, D. (1984) Illite: in *Micas,* S. W. Bailey, ed., Mineralogical Society of America, Reviews in Mineralogy **13,** 495–544.

Środoń, J., Morgan, D. J., Eslinger, E. V., Eberl, D. D., and Karlinger, M. R. (1986) Chemistry of illite/smectite and end-member illite: *Clays & Clay Minerals* **34,** 368–378.

Veblen, D. R. (1983) Exsolution and crystal chemistry of the sodium mica wonesite: *Amer. Mineral.* **68,** 554–565.

Woodland, B. J. (1985) Relationship of concretions and chlorite-muscovite porphyroblasts to the development of domainal cleavage in low-grade metamorphic deformed rocks from north-central Wales, Great Britain: *J. Struct. Geol.* **7,** 205–215.

Yau, Y.-C., Peacor, D. R., and Essene, E. J. (1987a) Hydrothermal treatment of smectite, illite and basalt to 460 °C: Comparison of natural with hydrothermally formed clay minerals: *Clays & Clay Minerals* **35,** 241–250.

Yau, Y.-C., Peacor, D. R., and Mcdowell, S. D. (1987b) Smectite to illite reaction in Salton Sea shales: A transmission and analytical electron microscopy study: *J. Sediment. Petrol.* **57,** 335–342.

Zen, E-an and Albee, A. L. (1964) Coexistent muscovite and paragonite in pelitic schists: *Amer. Mineral.* **49,** 904–925.

(Received 18 January 1993; accepted 8 February 1994; Ms. 2309)